

Properties of 17-4PH Steel

R. W. JUDY JR., C. T. FUJII AND
R. J. GOODE

*Strength of Metals Branch
Metallurgy Division*

December 18, 1973



NAVAL RESEARCH LABORATORY
Washington, D.C.

Approved for public release; distribution unlimited.

DOCUMENT CONTROL DATA - R & D

(Security classification of title, body of abstract and indexing annotation must be entered when the overall report is classified)

1. ORIGINATING ACTIVITY (Corporate author) Naval Research Laboratory Washington, D.C. 20375		2a. REPORT SECURITY CLASSIFICATION Unclassified	
		2b. GROUP	
3. REPORT TITLE PROPERTIES OF 17-4PH STEEL			
4. DESCRIPTIVE NOTES (Type of report and inclusive dates) Final report on one phase of a continuing NRL Problem.			
5. AUTHOR(S) (First name, middle initial, last name) R.W. Judy, Jr., C.T. Fujii, and R.J. Goode			
6. REPORT DATE December 18, 1973		7a. TOTAL NO. OF PAGES 24	7b. NO. OF REFS 15
8a. CONTRACT OR GRANT NO. NRL Problem M01-30		9a. ORIGINATOR'S REPORT NUMBER(S) NRL Report 7639	
b. PROJECT NO. 62755N-ZF54-544-002		9b. OTHER REPORT NO(S) (Any other numbers that may be assigned this report)	
c.			
d.			
10. DISTRIBUTION STATEMENT Approved for public release; distribution unlimited.			
11. SUPPLEMENTARY NOTES		12. SPONSORING MILITARY ACTIVITY Department of the Navy Chief of Naval Material Washington, D.C. 20360	
13. ABSTRACT <p>Most catastrophic structural failures are preceded by a period during which cracks and other defects grow by combined fatigue and environmental processes from relatively small sizes to a critical size, at which rapid fracture occurs. For applications in an aggressive environment, the factor that determines long-term reliability is the inherent sensitivity of the structural material to environmental crack growth. 17-4PH stainless steel was investigated for its fracture and stress corrosion cracking properties under both open circuit and cathodically coupled conditions. Established fracture mechanics test and interpretation procedures were used to determine the suitability of this material for use in the marine environment. The material was found to be sensitive to environmental cracking processes to such a degree that the characteristic K_{Isc} values for the conditions of cathodic coupling were extremely low for materials in the strength range of interest. Evidence of crack growth was found on the fractured surfaces of test specimens of 17-4PH steel. The conclusions of this investigation were that brittle fracture is not a problem for 17-4PH, but environmental crack growth is expected to cause maintenance problems for structures designed for long life.</p>			

14. KEY WORDS	LINK A		LINK B		LINK C	
	ROLE	WT	ROLE	WT	ROLE	WT
17-4PH steel Stress corrosion cracking Ratio analysis diagram Cathodic coupling						

CONTENTS

Abstract	ii
INTRODUCTION	1
GENERAL BACKGROUND OF TEST METHODS AND ANALYSIS PROCEDURES	1
Linear Elastic-Fracture Mechanics	3
Dynamic Tear Test	3
Graphical Fracture Mechanics	4
Ratio Analysis Diagram	6
Stress-Corrosion Cracking	8
MATERIALS AND PROCEDURES	11
Stress-Corrosion Cracking Tests	12
RESULTS	13
ACKNOWLEDGMENTS	18
REFERENCES	18

ABSTRACT

Most catastrophic structural failures are preceded by a period during which cracks and other defects grow by combined fatigue and environmental processes from relatively small sizes to a critical size, at which rapid fracture occurs. For applications in an aggressive environment, the factor that determines long-term reliability is the inherent sensitivity of the structural material to environmental crack growth. 17-4PH stainless steel was investigated for its fracture and stress corrosion cracking properties under both open circuit and cathodically coupled conditions. Established fracture mechanics test and interpretation procedures were used to determine the suitability of this material for use in the marine environment. The material was found to be sensitive to environmental cracking processes to such a degree that the characteristic K_{Isc} values for the conditions of cathodic coupling were extremely low for materials in the strength range of interest. Evidence of crack growth was found on the fractured surfaces of test specimens of 17-4PH steel. The conclusions of this investigation were that brittle fracture is not a problem for 17-4PH, but environmental crack growth is expected to cause maintenance problems for structures designed for long life.

Manuscript submitted July 26, 1973.

PROPERTIES OF 17-4PH STEEL

INTRODUCTION

Modern structures that must maintain a high degree of reliability for long service lifetimes in an aggressive environment can be designed only with modern fracture mechanics principles. Most structural failures are preceded by a period during which small defects and cracks grow to a critical size at which rapid fracture takes place. The principal causes of such failures are crack growth due to combined loading and environmental processes. Thus, for many applications the factor that dominates long-term reliability is the environmental sensitivity of the structural material, a property which is intrinsic to the material in a given environment. In many cases, low design stresses and/or frequent inspections can be utilized to circumvent environmental sensitivity; however, such methods result in a weight penalty on the one hand and excessive cost on the other, so that a more sensible course is to use materials of minimum sensitivity to environmental crack growth.

Precipitation-hardening stainless steels, and particularly 17-4PH, are being used in the sea-water environment, primarily in strut and foil systems for experimental hydrofoils. More importantly, it is proposed that 17-4PH should be used for similar applications in future fleet hydrofoils. However, in addition to the lack of a capability for field-weld repairs of 17-4PH steel parts, the material is known to be susceptible to subcritical crack growth. The severity of the crack growth problem can be defined only by the use of established fracture mechanics methods and analysis procedures. The research covered in this report explored the characteristics of 17-4PH steel and its expected structural performance in the sea-water environment.

GENERAL BACKGROUND OF TEST METHODS AND ANALYSIS PROCEDURES

Procedures for design to preclude all forms of crack extension due to environmental and loading effects become hopelessly complex if each item is considered individually. For this reason, it is necessary to have a system of interrelated material characterization parameters and an integrated analysis procedure to define the significance of all pertinent properties of various materials in the context of each particular application. The Ratio Analysis Diagram (RAD) system has been established specifically for this purpose [1 to 3]. In this section the test methods for defining material properties and the RAD systems and analysis procedures for interpreting the material characterizations in terms of structural performance are described.

The baseline parameter for design against structural failure is fast fracture. The full range of fracture states extends from glasslike brittleness to high levels of ductility; the important engineering reference points are the dividing lines or limits separating the three fracture states (Fig. 1):

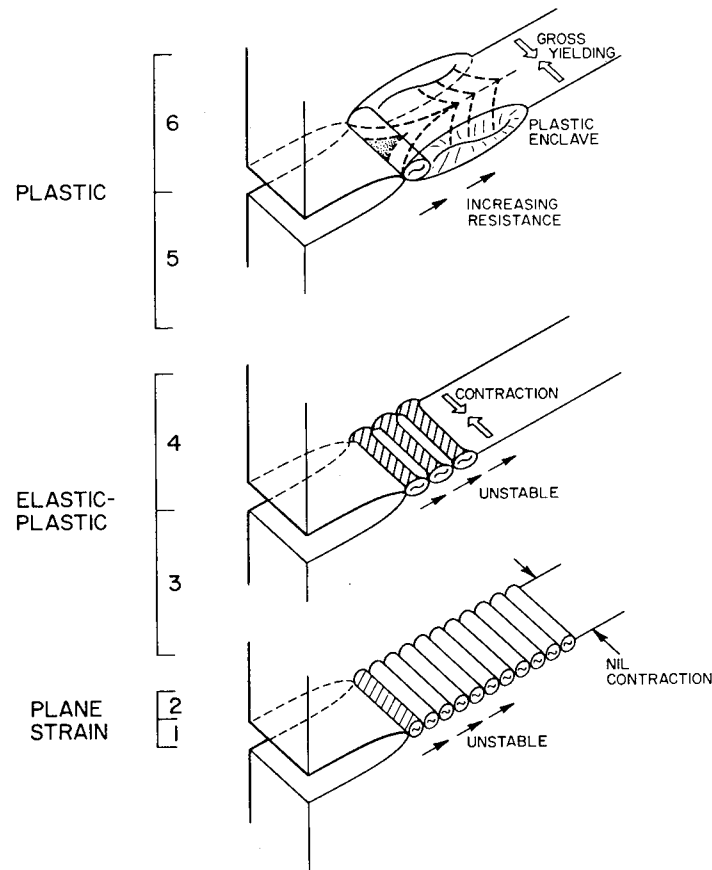


Fig. 1 — The three fracture states for high-strength metals

- Brittle behavior (plane strain), as illustrated at the bottom of the figure, can be viewed as the unstable propagation of cracks at energy levels that can be provided by elastic stress fields, with minimal attendant deformation or plasticity at the crack tip. Fracture states 1 and 2 refer to high and low levels of resistance to the initiation of unstable fractures.

- Crack extension in elastic-plastic conditions (middle figure) connotes crack propagation processes at high elastic stress levels with appreciable crack-tip plasticity. Fracture states 3 and 4 refer, respectively, to low and high elastic stress requirements for propagation of through-thickness cracks.

- Ductile (plastic) crack extension processes (top) involve stresses over yield, high crack-tip ductility, and consequent high energy expenditure to “drive” or enlarge the crack. Furthermore, in the first stages of crack extension, energy requirements to support crack growth increase rapidly, so that in the case of elastic stress fields a natural crack-arresting condition is present. Fracture states 5 and 6 refer, respectively, to low and high energy requirements to sustain stable crack extension at overyield stress levels.

The fracture state characteristics are defined by laboratory-type tests. The fracture state of a particular metal depends on the combination of metallurgical properties and mechanical constraint due to section size effects.

Linear Elastic-Fracture Mechanics

Linear elastic-fracture mechanics (LEFM) is a system for defining the relationship of crack size and stress level under conditions of plane strain. The plane-strain stress intensity, K_I , is a mechanical parameter which can be applied to design problems in the same manner as applied stress. Material properties are defined in terms of critical values of applied K ; for example, the parameter K_{Ic} describes the condition where fast fracture occurs. Another critical value of K is K_{Isc} , which is the applied stress intensity level for a material above which stress-corrosion cracking (SCC) will occur. The K_I parameter, which is always given in terms of $K_I = \alpha\sigma\sqrt{a}$, where σ = stress, a = crack length, and α is a term describing geometry effects, can be measured by different types of laboratory specimens (Fig. 2). A system of approved test methods for defining K_{Ic} has been established [4], and standardization procedures for K_{Isc} are currently being worked out. The basic requirement is that plane strain conditions must exist. To assure this, limits on the thickness of test pieces or structural components are $B \geq 2.5 (K_{Ic}/\sigma_{ys})^2$.

Dynamic Tear Test

The dynamic tear (DT) test was designed to measure the fracture resistance properties of structural materials for the entire range of strength and fracture resistance. The DT specimen is an edge-notched bend bar which is scaled dimensionally according to the thickness of the test material. Specimens are loaded dynamically to cause complete fracture; the index of performance is the energy required to fracture a standard specimen. There are two standardized test specimen configurations: 5/8-in. DT [5] and 1-in. DT [6] (Fig. 3). The range of thickness to which the test method applies is limited only by the size of available equipment; DT tests in the range of 0.25 in. to 12 in. in thickness have been conducted. Laboratory correlations of DT energy and K_{Ic} have been established for steels, titanium alloys, and aluminum alloys. These correlations permit use of the DT test in place of K_{Ic} tests so that LEFM analyses can be applied through the use of either of these tests.

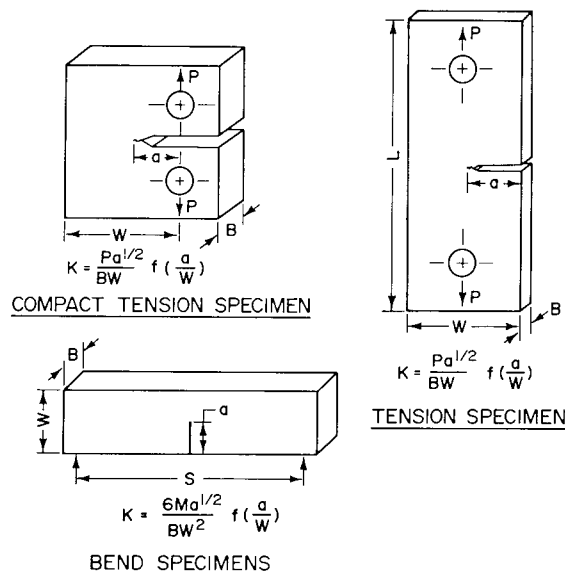
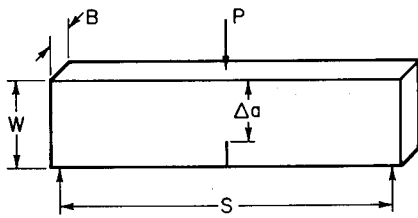


Fig. 2 — Specimen configurations for K_{Ic} tests



$$\text{ENERGY} = R_p B^x \Delta a^y$$

WHERE $R_p = \text{CONSTANT}$

Fig. 3 — Configurations of standard dynamic tear test specimens

STANDARD SPECIMENS

B		Δa		W		S	
(IN.)	(CM)	(IN.)	(CM)	(IN.)	(CM)	(IN.)	(CM)
0.63	1.6	1.125	2.9	1.625	4.1	6.5	16.5
1.0	2.5	3	7.6	4.75	12.1	16	41

Graphical Fracture Mechanics

Graphical Fracture Mechanics (GFM) plots are based on strict application of linear-elastic equations to depict the relations of stress levels and flaw sizes in tensile elastic stress fields. The premise is that fracture mechanics test specimens behave in a structure the same way as they do in the laboratory. Since the specimens serve as models, the equations apply only to those structures where the requirements of thickness, crack size and acuity, etc., are met. For different geometrical configurations there are several equations which can be used; two, however, have general applicability. The first is the surface-flaw equation, $K_{Ic} = 1.1 \sigma \sqrt{\pi a/Q}$, where K_{Ic} is the stress-intensity factor, σ the nominal tensile stress, a the crack depth, and Q the crack-geometry factor. The surface-flaw equation can be normalized by the yield strength σ_{ys} to allow reference to relative stress σ/σ_{ys} and to underscore that critical crack depth for a given stress depends only on the ratio K_{Ic}/σ_{ys} . This equation can be used to predict critical flaw depth for assumed geometries and stresses, as shown in Fig. 4, for the limiting cases of short flaws (approximately 3:1) and long, thin flaws (approximately 10:1), which bracket most of the natural crack geometries. The use of this chart is confined to section sizes for which the linear-elastic analysis applies, i.e., $B \geq 2.5 (K_{Ic}/\sigma_{ys})^2$. The B scale at the top of the figure and Table 1 reference this specification.

Another flaw type is a through-thickness crack, a type particularly applicable for thin-section materials. The equation is $K_{Ic} = \sigma \sqrt{\pi \ell/2}$, where ℓ = length of the through crack. The limits on strict applicability of this equation are the same as for surface cracks, as is shown in Fig. 5 for the 1-in. thickness. The equation applies in the plane-strain region, which is bounded by the plane-strain limit, but not to the elastic-plastic and plastic regions above this limit. The boundary between plastic and elastic-plastic regimes, given by $B = (K_{Ic}/\sigma_{ys})^2$, corresponds to the point where $\sigma/\sigma_{ys} = 1$. The intercept on the plane-strain limit line is relatively insensitive to crack length, so that the curves for all cracks designated 2T (2 × thickness) to 6T are at approximately the same low stress level (less than half yield at the plane-strain limit). In general, surface cracks in plane-strain materials require high stresses ($\sigma/\sigma_{ys} = 0.8$ or more) to cause fracture extension, but through-thickness cracks become unstable at values of σ/σ_{ys} of 0.3 to 0.5, which is very near allowed values for most design applications.

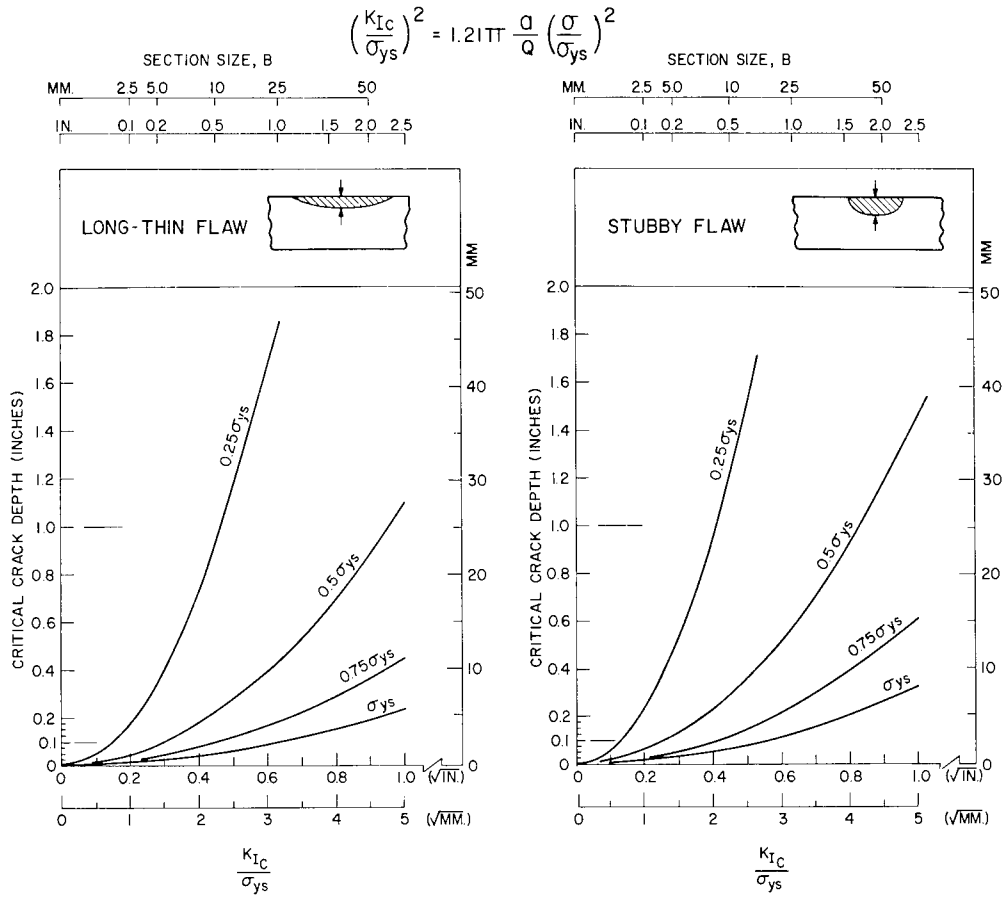


Fig. 4 — Graphical fracture mechanics plots of surface cracks for two flaw shapes

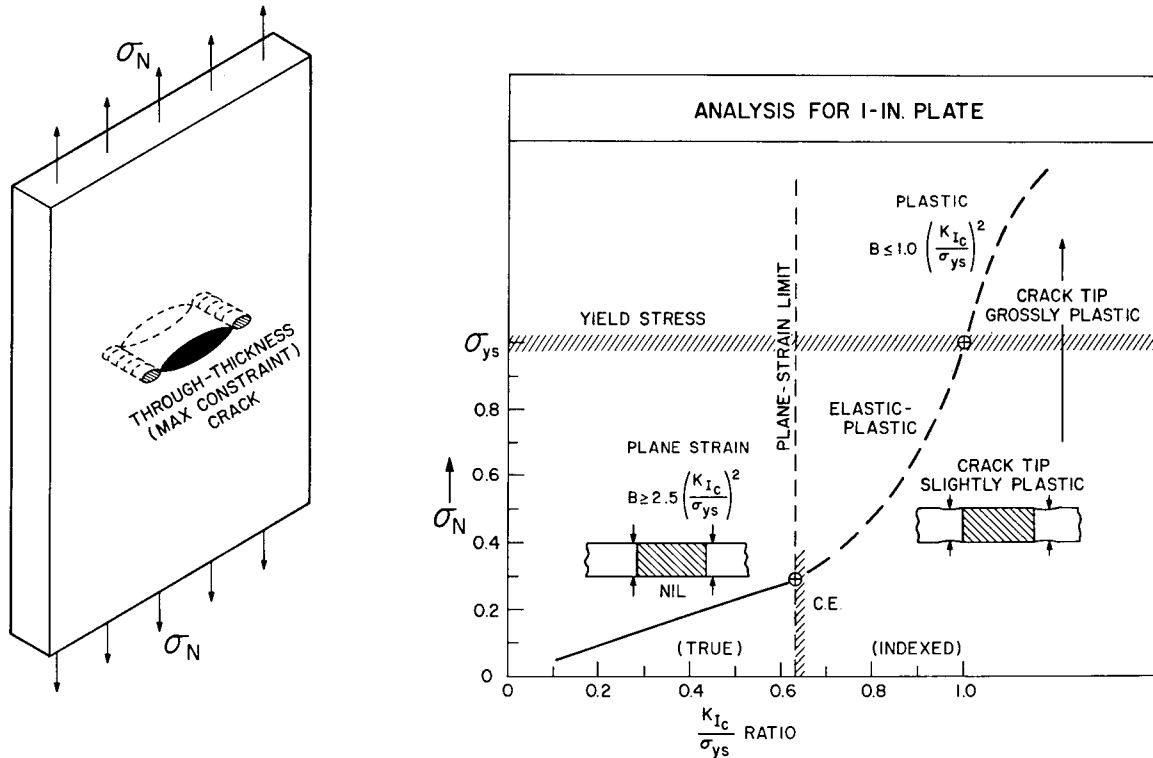


Fig. 5 — Graphical fracture mechanics plot for through-thickness crack

Ratio Analysis Diagram

The RAD provides a format for analysis of the fracture resistance of structural materials over the entire range of strength and fracture resistance. RAD's have been developed for steels, titanium, and aluminum alloys [7].

The RAD framework is formed from the scales of yield strength vs K_{Ic} and DT energy, as shown in Fig. 6. The most prominent features of the RAD are the limit lines and the system of lines of constant K_{Ic}/σ_{ys} ratio. The technological limit (TL) line represents the highest values of fracture resistance measured to date, either by DT tests over the entire yield-strength range, or by K_{Ic} tests in the elastic-fracture range; the lower bound represents the lowest levels of fracture resistance. Reference to the critical flaw size charts, Figs. 4 and 5, is provided by the system of ratio lines constructed from the scales of K_{Ic} and σ_{ys} . As an example, critical sizes for a long, thin surface flaw for half-yield and full-yield loading conditions are shown on the RAD for each ratio line.

The ratio lines also divide the diagram into regions of expected plastic, brittle, and elastic-plastic behavior for given material thicknesses. The separations are determined according to thickness, as shown for a 1-in. section size in Fig. 6. The critical edge between brittle behavior and elastic-plastic behavior is the plane-strain limit. The boundary between the elastic-plastic and ductile regimes is the general yield limit. Table 1 contains both plane-strain limits and general yield limits as related to section size. The division of the RAD into three regions provides an engineering index of the fracture state and thereby serves to indicate the type of more detailed design approach required for each case.

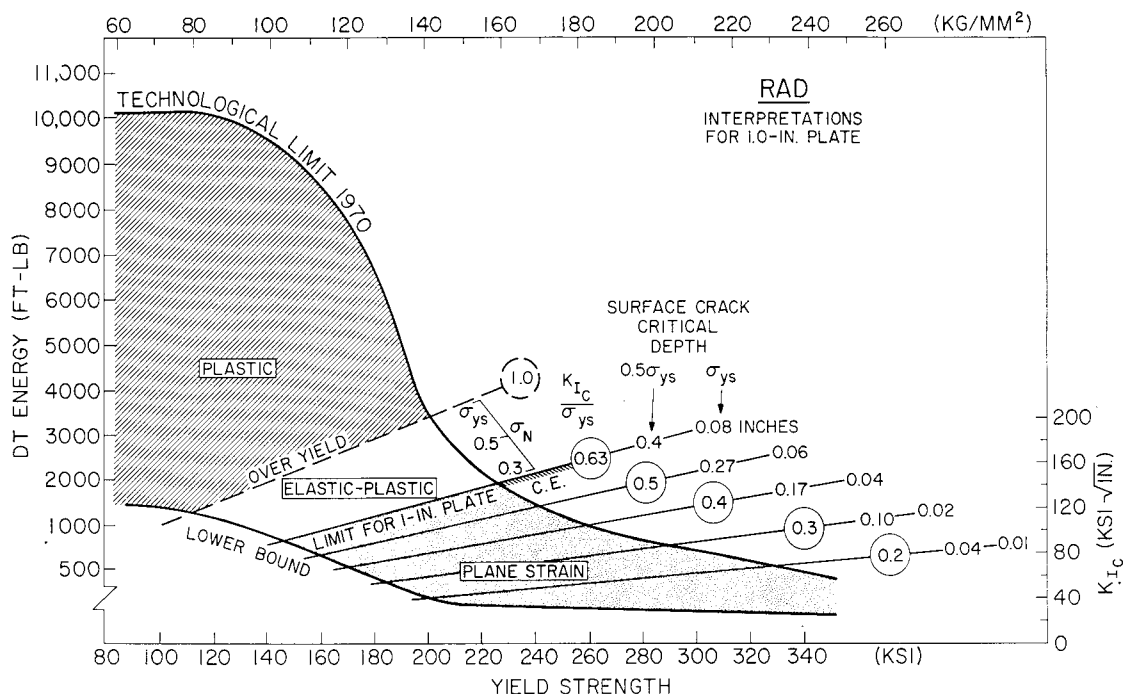


Fig. 6 — Ratio analysis diagram for steels

Table 1
Limits of Applicability of Linear Elastic Fracture Mechanics

Section Size	Plane-Strain Limit K_{Ic}/σ_{ys} (ksi)	General Yield Limit $\frac{\sigma_{ys}}{\text{ksi}\sqrt{\text{in.}}/\text{ksi}}$
0.1	0.20	0.32
0.2	0.28	0.45
0.3	0.35	0.55
0.4	0.40	0.63
0.5	0.45	0.71
1.0	0.63	1.0
1.5	0.8	1.21
2.0	0.9	1.41
3.0	1.1	1.73
6.0	1.5	2.45
10.0	2.0	3.17

The RAD is a “plotting board” for analysis of combined strength and fracture resistance properties of materials in relation to specific structural mechanics problems. Effects of the variability of materials properties and minimum strength specifications for particular structures are readily analyzable. Of particular importance is the strength transition effect, which is the rapid decrease of fracture resistance in narrow ranges of yield strength; this decrease is depicted by the TL line. Additionally, effects of crack growth due to fatigue and SCC processes are made readily apparent by RAD procedures [8].

Stress-Corrosion Cracking

In addition to basic stress-analysis procedures, a structural designer must consider the effects of loading and environment that cause existing flaws to grow to critical sizes. One of the primary problem areas for structures that operate in hostile environments is the growth of flaws by stress-corrosion cracking (SCC). There are several mechanisms by which cracks grow under the combined effects of active environments and applied stresses; however, the macroscopic effect is crack propagation, which is designated SCC for engineering purposes.

The susceptibility of structural metals to SCC is not predictable from mechanical property data; the only way to determine a material's relative sensitivity to environmental effects is to conduct laboratory tests. Sharp-crack fracture mechanics procedures have been extensively used for this purpose.

Structural failures due to corrosion and stress-corrosion factors generally occur in the following three distinct phases, which are depicted in Fig. 7.

1. Pitting corrosion is the formation of small pits by localized electrochemical processes. Once formed, pits grow by a combination of fatigue and localized corrosion to a size at which cracking begins and SCC processes take effect.
2. Stress-corrosion cracking is the propagation of a crack due to the combined influence of the environment and the stress field.
3. Final failure by either unstable brittle fracture or ductile, overload fracture results from the growth of the crack to a size that is critical for the imposed stress level.

Designers are concerned primarily with phases 2 and 3 of the process, i.e., the important factors are SCC and the manner of final failure. Phase 1 can be excluded from a practical standpoint because many structures have cracks which are larger than most of the corrosion pits that are present. Design against failure by SCC therefore requires either precluding rapid SCC propagation by selecting resistant materials or predicting the rate of crack propagation and the conditions for final fracture to assure a safe operating period.

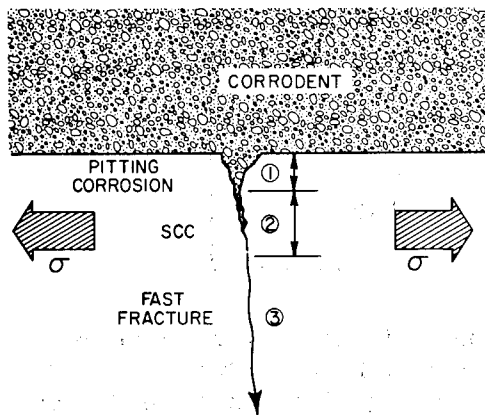


Fig. 7 — Three stages of crack extension leading to structural failure due to stress corrosion. The pitting stage is eliminated in the presence of preexisting cracks.

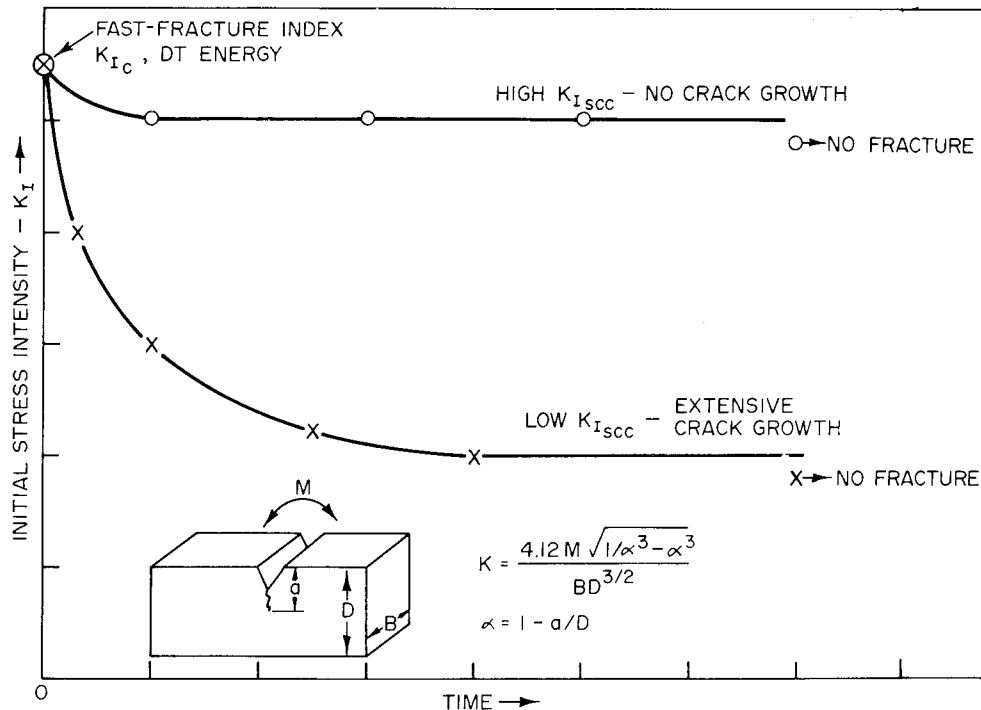


Fig. 8 — Typical plots of applied K vs time for high and low $K_{I_{SCC}}$ materials. Plots of this type are used for determining characteristic $K_{I_{SCC}}$ values. The cantilever specimen configuration is also shown.

A threshold effect in SCC behavior exists for structural materials. The threshold is dependent on K and is *independent of applied stress*. The characteristic K value at the threshold, called $K_{I_{SCC}}$, defines the level of applied K above which SCC will occur if the material is sensitive to environmental effects.

The fatigue-cracked cantilever test specimen [9] and schematic data plots for a SCC sensitive material and an insensitive material are shown in Fig. 8. The $K_{I_{SCC}}$ value is determined by bracketing methods for specimens which experience SCC and eventual fracture and for specimens which do not fracture for a specified time period. Low values of $K_{I_{SCC}}$ relative to the fast-fracture index point (K_{Ic} or DT), which is plotted at time zero for reference, indicate that crack growth occurs before the fracture. Values of $K_{I_{SCC}}$ near the fast-fracture index are evidence that there is no crack growth and that fracture is caused by simple overload and yielding processes. On a display of this type (Fig. 8), time is not an important factor since the fracture time depends on the geometry of the specimen and the initial K_I level.

A more accurate picture of the events of a $K_{I_{SCC}}$ test is shown in Fig. 9, which is a replot of the SCC sensitive material of Fig. 8 on the same coordinate system. In the cantilever test, identical test specimens are loaded over a range of *initial* values of applied K , and the cracks are allowed to grow until the specimen fractures. Since the load is constant, the applied K level increases with crack growth until the fast-fracture index is reached. Therefore, if the initial stress intensity is high (high load), a small amount of crack growth is sufficient to cause fracture; conversely, a low initial stress intensity allows for a large crack-growth increment and a long time to fracture. The no-fracture specimens do not

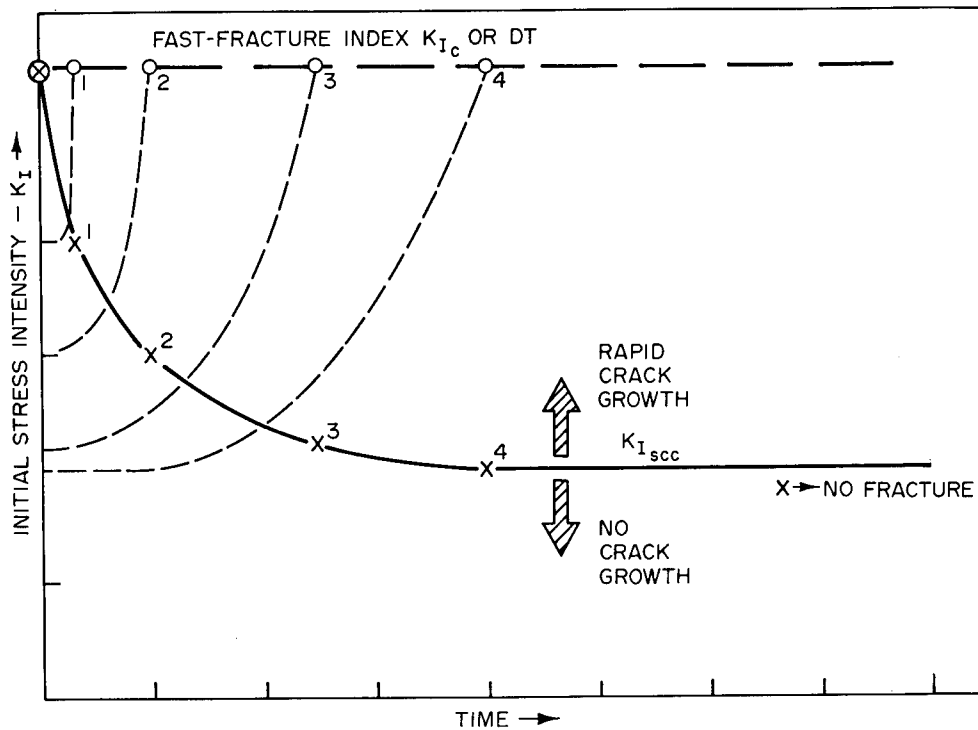


Fig. 9 — Crack growth in relation to K_I and time. The amount of crack growth in a test specimen depends on both the initial K_I value and the fast-fracture index, as shown. The crack begins to grow at time zero, and continues to grow until the applied K level increases to the fast-fracture index. The numbers by the data points correspond to the crack growth curves.

have crack growth; these specimens are used to set a lower limit on K_{Isc} . Use of the time scale in design is impossible because of the geometry dependence of crack growth on the level of K required to fracture the specimen. The significant factor is the K_{Isc} threshold value which separates the region of rapid crack growth from the region of no crack growth. The necessity to have positive evidence of crack growth to give validity to K_{Isc} values is often overlooked. In many cases where fracture toughness is low, values of K_I are measured and reported as K_{Isc} , when in fact, no cracking processes other than fast fracture are present.

The effects of electrochemical coupling of test material with other metals, as might be found in galvanic ship protection systems, are either to increase or decrease crack-growth rates or, more importantly, to increase or decrease K_{Isc} , depending on the applied potential. The effect of potential on K_{Isc} is the dominant factor, since this controls the presence (or absence) of crack growth.

The advantage of using stress-intensity parameters to define SCC properties is that the K_{Isc} value can be used in conjunction with the same equations and criteria that apply to fracture to determine flaw-size/stress-level conditions necessary for crack growth to begin. For proper use of linear-elastic fracture principles to characterize SCC properties of structural metals, plane-strain conditions must dominate the stress state because LEFM is only concerned with plane strain.

The SCC resistance of a material is determined by comparison of the critical flaw size for fast fracture with the critical flaw size for SCC propagation which will eventually lead to fast fracture. This can be done for plane-strain materials by comparing $K_{I_{SCC}}$ with K_{I_C} . The $K_{I_{SCC}}$ parameter by itself does not denote whether or not the material is sensitive to the environment, because $K_{I_{SCC}}$ values cannot be larger than K_{I_C} ; i.e., materials with low K_{I_C} values will always be limited to low values of $K_{I_{SCC}}$. For ductile materials, comparison of the $K_{I_{SCC}}$ value must be made with some other index of fast-fracture resistance such as DT or R-curve analyses. A third possibility is the case where a valid $K_{I_{SCC}}$ cannot be measured. This condition denotes that the thickness is insufficient to maintain the plane-strain state; i.e., that the material, at that thickness, would not be highly sensitive to SCC.

The primary effect of SCC on structural design is to lower the flaw tolerance of a material, not by changing the intrinsic resistance to fast fracture, but by changing the critical condition for failure. Failure processes for materials sensitive to SCC usually occur at plane-strain tolerance levels, a fact which implies that RAD procedures can be adapted to analyze effects of SCC. SCC characterizations of structural materials can be entered on the RAD via existing K_{I_C} scales; this procedure permits direct comparison of conditions for fast fracture and SCC.

In the practical sense, the ability to utilize LEFM is of marginal value except for applications where very short life structures are involved, and where loads are known precisely, because the designer is faced with proving that the flaw-size/stress-level combination necessary to have an applied K_I equal to or above $K_{I_{SCC}}$ does *not* exist. To use materials of low $K_{I_{SCC}}$ values for structures with long expected lifetimes, it is necessary to predict the following:

- the size of the initial flaw;
- the size of flaw that would cause final failure;
- the rate of crack growth in the structure under expected load cycles; interrelationships of SCC, fatigue, and corrosion-fatigue effects are involved;
- proper inspection procedures and intervals to monitor flaw growth and the remaining safe life of the structure.

For long lifetime structures, where loads are not known precisely, the only question to be addressed is whether a material that is sensitive to environmental effects in the form of accelerated crack growth can be accepted. A more judicious approach is to preclude the use of materials that are sensitive to SCC in critical applications; then the problem is reduced to whether SCC is present or not.

MATERIALS AND PROCEDURES

The test materials were three plates of 17-4PH stainless steel. Plates 1 and 2 were 1/2 in. thick and 1 in. thick, respectively, and were produced by argon-oxygen melting (air-melt) practices. The third material was a plate 1 in. thick produced by vacuum-melt practice. All test plates were received in the annealed condition. After DT and tensile tests revealed inferior properties, tests of the air-melt plates were discontinued.

The following tests were conducted for the vacuum-melted 1 in. thick plate:

- Tensile tests (0.505 in. diameter)
- Full-thickness DT tests
- Open-circuit $K_{I_{sc}}$ tests
- $K_{I_{sc}}$ tests at various electrochemical potentials to simulate cathodic coupling to other metals.

All test samples were heat-treated to attain a range of yield strength so that optimum strength/fracture resistance levels could be defined. The heat treatment schedules are given in the tables of test results. Dynamic tear tests of all plates were conducted in full thickness in each heat-treated condition. Specimen dimensions are as shown in Fig. 3; duplicate specimens were tested at each heat-treated condition.

Stress-Corrosion Cracking Tests

SCC test specimens were cut from the vacuum-melted, 1-in.-thick plate of 17-4PH steel. The cantilever test method was used to measure stress-intensity factors in air (K_{I_x}) and in salt water ($K_{I_{sc}}$) for different strength levels of the material. The dimensions for the SCC specimens, as-machined, were: $B = 0.75$ in., $B_n = 0.70$ in., and $D = 1.0$ in. (see Fig. 8). The dimension B_n is defined as the breadth as reduced by side grooves. A correction factor [10] was applied to the measured K_I value to compensate for the side grooves.

Initially, the approximate stress-intensity factor in air, K_{I_x} , was determined for each strength level to serve as a baseline for measuring the effects of salt water and cathodic polarization. For the SCC tests the corrodent was a 3-1/2% NaCl solution (3.5 g NaCl per 100 ml. distilled water) contained in a polyethylene reservoir around the crack. One series of experiments in sea water was performed earlier at the NRL Marine Corrosion Laboratory at Key West, Florida [11]. To establish $K_{I_{sc}}$, a step-load, bracketing technique was used as outlined below.

1. Initial load — 50% of K_{I_x} ; Increase load $10 \text{ ksi}\sqrt{\text{in.}}$ every 24 hours until specimen breaks.
2. Initial load — $15 \text{ ksi}\sqrt{\text{in.}}$ below K_I , the break value from step 1; Increase load $10 \text{ ksi}\sqrt{\text{in.}}$ every 100 hours until break.
3. Initial load — $5 \text{ ksi}\sqrt{\text{in.}}$ below K_I , the break value from step 2; Increase load $10 \text{ ksi}\sqrt{\text{in.}}$ every 100 hours until break.

The $K_{I_{sc}}$ value falls between the lowest K_I value from a fractured specimen and the highest no-break K_I value attained from the *initial* load.

Indications of crack growth were obtained by noting the movement of the cantilever beam as detected by a precision dial gauge positioned near the loaded end of the beam. Upon completion of the SCC test, crack growth was verified by visual and microscopic examination of the fracture surfaces.

In subsequent separate tests to establish cathodic polarization effects, 5086 aluminum alloy, zinc, and magnesium anodes comparable in area to that of the immersed portion of the specimen were coupled to the specimen. In all of the SCC tests the electrochemical potentials of the specimens were measured against a Ag/AgCl reference electrode.

RESULTS

The results of the DT and tensile tests for the air-melted and vacuum-melted material are reported in Tables 2 and 3, respectively. The data for DT tests of the 1/2-in.-thick air-melted plate are plotted on the RAD in Fig. 10, using the scale of R_p to locate the energy values measured with nonstandard specimens [12]. Note that the data follow the lowest possible levels of fast-fracture resistance. For this reason, the 1/2-in.-thick, air-melted 17-4PH steel was not included in further studies. Data showing the fast-fracture properties of the 1-in.-thick plates, both air-melted and vacuum-melted, are shown on the RAD in Fig. 11. In both cases, the fracture resistance is very low at approximately 180 ksi yield strength and increases rapidly at lower values of yield strength. However, the fast-fracture properties of the vacuum-melted plate were higher than those of the air-melted plate, so that further tests were conducted only on the vacuum-melted plate. The results of the SCC tests on specimens cut from this vacuum-melted plate are summarized in Table 4.

Zones showing the fracture and SCC properties of the vacuum-melted 17-4PH steel are presented on the RAD in Fig. 12. The fast-fracture properties are indicated in the DT zone, the open circuit SCC properties by the SCC zone, and the electrochemical coupling effects by the cathodic couple zone. SCC data from other sources (Table 5) were also used to delineate the SCC zone shown on this diagram. So that the zones would not overlap to a degree that would cause confusion, the rapid decrease of fast-fracture resistance at 180-ksi yield strength is not depicted by the DT zone. All other zones, however, conform to the data populations.

Table 2
Mechanical Properties of Air-Melted 17-4PH Steel

Thickness	Condition	DTE (ft-lb)	σ_{ys} (ksi)	σ_{ts} (ksi)	El (%)	RA (%)
1-in. plate	H900	475	181.4	202.3	15	49
	H975	1500	170.5	179.3	16	53
	H1028	1930	165.2	171.6	15	52
	H1075	2735	152.1	160.4	17	54
	H1150	4205	99.0	144.5	19	58
1/2-in. plate	H900	240*	182.6	208.0	14	44
	H975	315	169.4	182.2	13	48
	H1050	795	160.3	167.1	14	50
	H1100	1160	153.8	160.7	14	51
	H1150	1710	130.0	148.2	16	52

*Equivalent 1-in. DTE calculated from $E = R_p B^{1/2} \Delta a^2$.

Table 3
Mechanical Properties of Vacuum-Melted 17-4PH Steel

Condition	DTE (ft-lb)	σ_{ys} (ksi)	σ_{ts} (ksi)	El (%)	RA (%)
H900	320	177.0	195.6	14	50
H975	2510	161.7	170.8	15	55
H1025	3335	156.6	162.4	15	55
H1075	3175	150.9	156.5	17	55
H1150	4815	120.3	141.6	19	61
H1150M		91.0	124.6	22	64

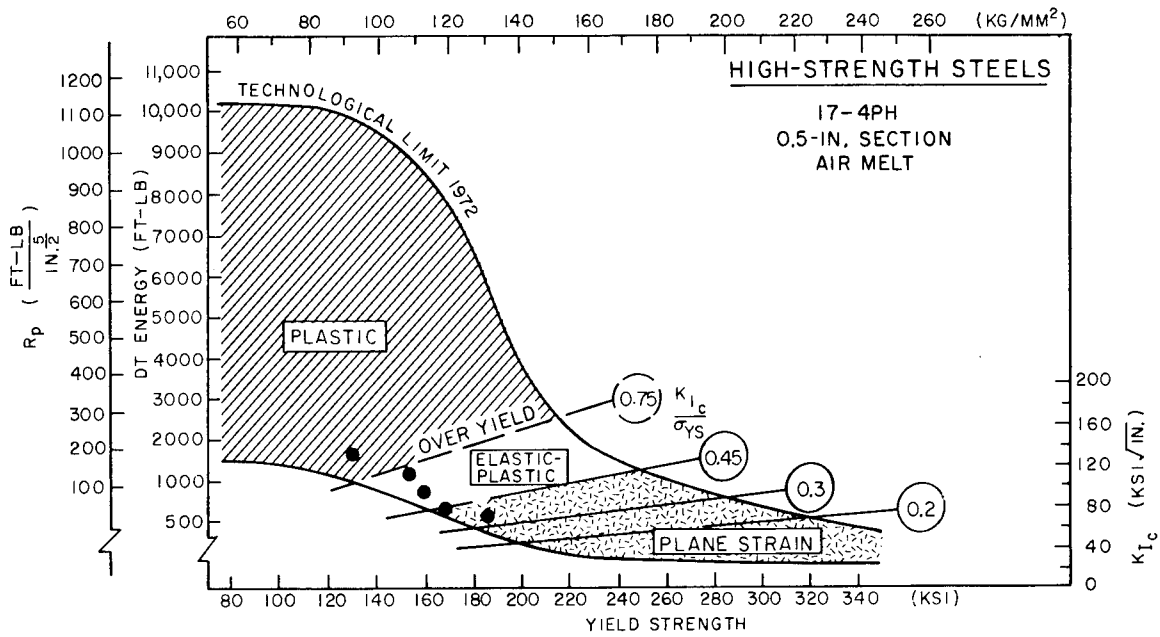


Fig. 10 — RAD showing data for 0.5-in. air-melted 17-4PH steel

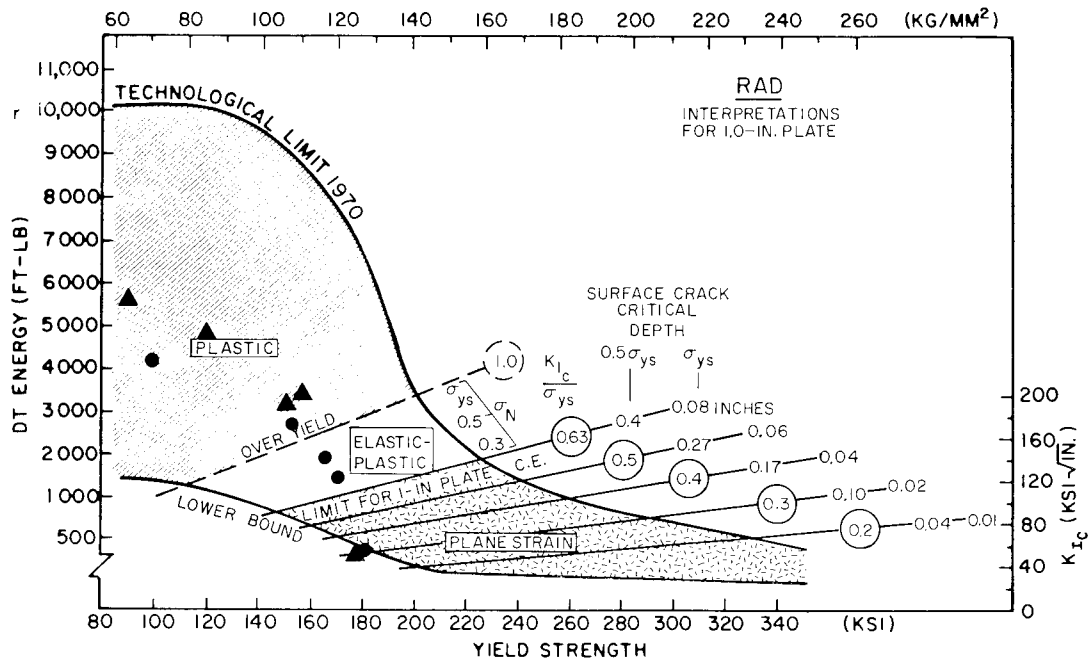


Fig. 11 — RAD showing data for 1.0-in. plates of 17-4PH steel, vacuum-melted (triangles) and air-melted (circles)

Table 4
SCC Properties of Vacuum-Melted 17-4PH Steel in 3-1/2% NaCl

Condition	K _{Isc} (ksi√in.)				Remarks
	Open Circuit	Coupled			
		Al	Zn	Mg	
H900	45	36	30	17	Natural seawater
H925	82	73	45	20	Synthetic seawater
H1075	117	103	59	49	Synthetic seawater
H1150	124	105	74	52	Synthetic seawater
H1150M	97	93	88	90	Synthetic seawater

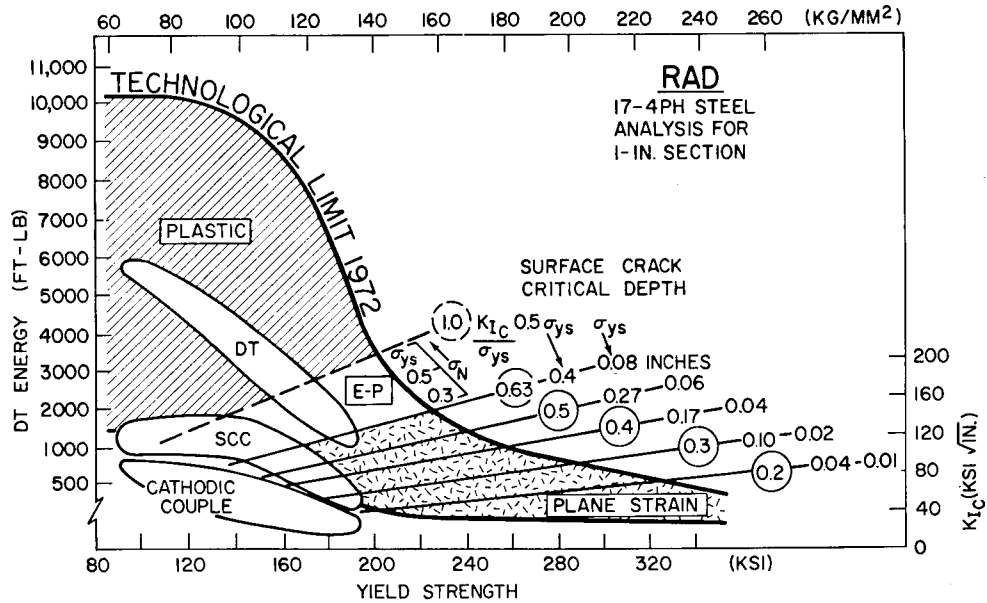


Fig. 12 — Zones showing fracture, SCC, and cathodically coupled SCC properties of vacuum-melted 17-4PH steel. See text for details.

Table 5
SCC Data from Other Sources

Condition	σ_{ys} (ksi)	$K_{I_{sc}}$ (Ksi√in.)			Reference
		Open Circuit	Coupled		
			Al	Zn	
H900	180	47	50	33	13
H1000	150	92	71	49	
H900	177	52	28	—	14, 15
H1000	158	119	91	—	

Except for the high strength end of the data zone, fast fracture of vacuum-melted 17-4PH steel is not expected to be a problem. For the materials in the plastic region (yield strength less than 160 ksi), reasonable size flaws (3T) and stresses over the yield strength would be required to cause fracture extension. For most applications where such loading conditions are expected only infrequently and flaws are expected to be small, this is an adequate level of fracture resistance. However, the preceding conditions represent the base-plate property under short-time loading; in applications involving the 17-4PH steel, the effects of time, stress, and environment on the integrity of structures are of more concern.

Stress-corrosion cracking tests at open circuit and with various levels of applied potential to simulate electrochemical coupling with other metals revealed a definite susceptibility

of the 17-4PH alloy to SCC. This means simply that the cracks and other defects which exist in most structures, particularly welded structures, will grow when the applied crack-tip stress intensity exceeds the $K_{I_{SCC}}$ value measured for the applicable conditions. The location of the SCC zone in the plane strain region well below the DT zone is clear evidence that cracks are expected to grow. Corroborating evidence is provided by electron microscope examination of fracture surfaces from SCC test specimens that showed a cleavage fracture mode in the crack-growth region (Fig. 13). Cleavage fracture in this steel is evidence of SCC; the microvoid coalescence or dimpled rupture shown in Fig. 13 for the fast-fracture area of the test specimen is typical for ductile materials. It is especially important to note that crack growth was found in all cases, whether valid, plane strain $K_{I_{SCC}}$ numbers were obtained from the tests or not. Although accurate calculations of critical conditions for fracture cannot be made from the non-plane-strain K values, crack growth can be expected at reasonably high stress levels.

The worst condition for use of 17-4PH steel is where a cathodic-couple exists. The same factors apply as for open-circuit conditions except that the $K_{I_{SCC}}$ numbers measured under these conditions are extremely low for materials of the 130-170 ksi strength range. RAD analysis predicts that for a $K_{I_{SCC}}/\sigma_{ys}$ ratio of 0.2 (which is the lower limit) crack growth can begin at flaws 0.040 in. deep at stresses of half yield. At stresses of 1/4 yield, crack growth can begin from a flaw depth of 0.15 in. The flaws can grow to quite large sizes because of the elastic-plastic and plastic fracture resistance levels of the material in the yield-strength range below 160 ksi; however, it is important to note that increased crack size due to other factors can lead to crack growth at lower stress levels. This is because K_I increases both with increased stress and with greater crack size. Thus, once SCC propagation has begun, the probabilities of crack arrest are remote. The likelihood of finding SCC cracks in routine inspections is also very low because such cracks can grow without apparent surface penetration.

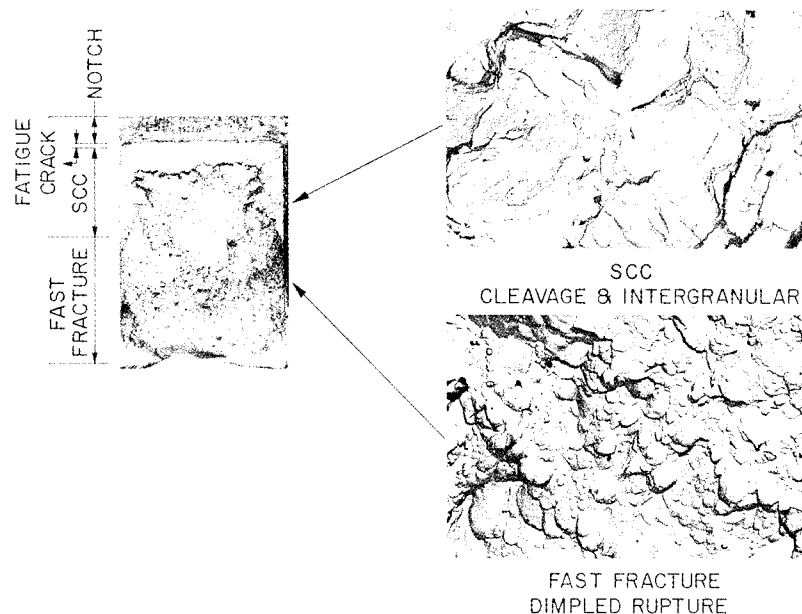


Fig. 13 — Fracture modes for SCC and fast fracture of cantilever test specimen

Many of the problems associated with use of 17-4PH as well as other high-strength steel systems can be attributed to the fact that they are transitional with respect to flaw tolerance parameters and yield strength. The decrease in fracture resistance with increasing σ_{ys} , as shown by the DT zone of Fig. 12, would also be expected for the low-strength end of the SCC and cathodic couple zones if the K_{Isc} values could be measured accurately. This is not possible, however, because of section size effects. Use of 17-4PH steel for any application thus requires selection of both minimum and maximum yield strength limits necessary to preclude fracture problems. The crack-growth problem is less severe at low yield-strength levels because the flaw tolerance is higher and because the combined stress/flaw-size condition necessary to cause SCC increases as yield strength decreases.

It must also be observed that the analyses in this report have been confined to 1-in. section materials. Use of 17-4PH in heavy sections (2 to 3 in. or greater in thickness) would move the plane-strain limit to higher levels and thereby decrease the allowable maximum yield strength necessary to avoid brittle fracture. A simple calculation shows that for 3-in. thickness the plane strain limit is $K_I/\sigma_{ys} = 1.10$; the corresponding maximum allowable σ_{ys} is approximately 150 ksi. In 3-in.-thick material, SCC characteristics would be the same as for 1.0-in. plate at yield-strength levels of approximately 150 ksi or greater; at lower yield-strength levels SCC problems would be more severe than those expected for 1.0-in. plate because of the existence of plane-strain conditions in the thicker material.

ACKNOWLEDGMENTS

The authors gratefully acknowledge the contributions of Messrs. W.E. King, Jr., and R.L. Newbegin for specimen preparation and experimental assistance and the Chief of Naval Material for providing the financial support for the research studies of this report.

REFERENCES

1. W.S. Pellini, "Criteria for Fracture Control Plans," NRL Report 7406, May 11, 1972.
2. W.S. Pellini, "Integration of Analytical Procedures for Fracture-Safe Design of Metal Structures," NRL Report 7251, Mar. 26, 1971.
3. W.S. Pellini, "Advances in Fracture Toughness Characterization Procedures and in Quantitative Interpretations to Fracture-Safe Design for Structural Steels," Welding Research Council Bulletin 130, May 1968; also NRL Report 6713, Apr. 3, 1968.
4. "Standard Method of Test for Plane-Strain Fracture Toughness of Metallic Materials," ASTM Standard E399-72 Annual Book of ASTM Standards, Part 31, July 1972, p. 955.
5. E.A. Lange, P.P. Puzak, and L.A. Cooley, "Standard Method for the 5/8-Inch Dynamic Tear Test," NRL Report 7159, Aug. 27, 1970.
6. P.P. Puzak and E.A. Lange, "Standard Method for the 1-Inch Dynamic Tear Test," NRL Report 6851, Feb. 13, 1969.
7. R.J. Goode and R.W. Judy, Jr., "Fracture-Safe Design of Aluminum and Titanium Alloy Structures," NRL Report 7281, Feb. 14, 1972.
8. R.W. Judy, Jr., and R.J. Goode, "Stress-Corrosion Cracking of High-Strength Steels and Titanium Alloys," *Welding J.* 51 (No. 9), 437 (Sept. 1972).

9. B.F. Brown, "A New Stress-Corrosion Cracking Test for High-Strength Alloys," *Materials Research and Standards* 6 (No. 3), p. 129 (1966).
10. C.N. Freed and J.M. Krafft, "Effect of Side Grooving on Measurements of Plane-Strain Fracture Toughness," *J. Mat.* 1 (Nov. 4), 770 (1966).
11. T.J. Lennox, Jr., R.E. Groover, and M.H. Peterson, "How Effective is Cathodic Protection of Stainless Steels in Quiescent Sea Water?" *Materials Protection* 8 (No. 5), 41 (1969).
12. R.W. Judy, Jr., and R.J. Goode, "Ductile Fracture Equation for High-Strength Structural Metals," *NRL Report 7557*, Apr. 3, 1973.
13. G.J. Biefer and J.G. Garrison, "Stress-Corrosion Cracking Tests on Some High-Strength Steels Using the U.S.N. Cantilever Method," *Internal Report PM-R-67-8*, Physical Metallurgy Division, Dept. of Energy, Mines and Resources, Ottawa, Canada, Mar. 14, 1967.
14. C.S. Carter, D.G. Farwick, A.M. Ross, and J.M. Uchida, "Stress Corrosion Properties of High Strength Precipitation Hardening Stainless Steels," *Corrosion* 27, p. 190, 1971.
15. C.S. Carter, "The Effect of Aluminum Coupling on the Fracture Resistance of 17-4PH and 15-5PH Steels in Aqueous Solution," *Boeing Document D6-25219*, April 1971.